Geopersia 2024, 14(2): 439-452
DOI: 10.22059/GEOPE.2024.379254.648761

RESEARCH PAPER

An Integrated Approach for 3D Facies Modeling of Kangan and Dalan Reservoirs, South Pars Gas Field, Persian Gulf

Ebrahim Sfidari [1,*], Javad Amraie [2], Houshang Mehrabi [1], Seyed Mohammad Zamanzadeh [3]

[1] Petroleum geology research group, Research Institute of Applied Sciences, Tehran, Iran
[2] Research and Technology Division, National Iranian Oil Company (NIOC) , Tehran, Iran
[3] Department of Geology, College of Sciences, University of Tehran, Tehran, Iran

Received: 11 July 2024, Revised: 29 July 2024, Accepted: 02 August 2024

Abstract
This study focuses on the facies modeling and reservoir characterization of the Permian-Triassic age Dalan and Kangan formations, defined as the main reservoirs in the Persian Gulf's South Pars Gas Field. Based on the main characteristics of petrographical observations, 12 facies were identified and classified into four facies associations representing tidal flat (LFAs 1), lagoon (LFAs 2), shoal (LFAs 3), and open marine (LFAs 4) conditions on a carbonate ramp. A neural network approach (self-organizing maps) was employed to predict lithofacies and lithofacies associations (LFAs) in uncored wells. The method demonstrated a high level of accuracy, achieving an 87.5% success rate in predicting lithofacies using GR, DT, NPHI, RHOB, and PEF logs. The predicted LFAs were compared with the core-derived facies and rock types to generate a 2D facies model within the sequence stratigraphy framework for geologic modeling and subsequent reservoir simulation. Finally, geostatistical techniques were employed to prepare a 3D facies distribution and depositional model for the entire field. The stochastic simulation method was applied here to simulate and generate the 3D model of four major LFAs involved in the modeling. Facies modeling of the formations indicates a gentle shallowing from zone K4 to zone K3. The connectivity of LFAs 3 is well observed in zone K4, whereas in zone K3 the connectivity of LFAs 2 is evident. Zone K2 is associated with dominant LFAs 3 and minor LFAs 4. The zone K1 is characterized by the dominance of LFAs 1.

Keywords: Lithofacies, Log facies, Reservoir simulation, Carbonate reservoir, South Pars Gas Field, Persian Gulf.

Introduction

Opening of the NW-SE trending Neo Tethys Ocean followed by regional movement of the Qatar Arch resulted in the development of a wide carbonate ramp in the north margin of the Arabian Plate, in which deposition of shallow marine carbonates of Kangan and Dalan formations took place during Permian to the Triassic period in Iran (or Khuff Formation in the Arabian plate) (Ghazban, 2007; Kalhor et al., 2024). These formations are the main reservoirs of the giant South Pars Gas Field (SPGF) (Fig.1).

The carbonate facies of the Kangan and upper Dalan formations in the studied area are classified into 4 reservoir units, known as K1, K2, K3 and K4 (from top to base) (e.g., Alsharhan, 1993; Sharland et al., 2001; Insalaco et al, 2006; Ehrenberg et al, 2007; Rahimpour-Bonab et al, 2009, Sfidari et al, 2012; Shahkaram et al, 2022; Moradi et al. 2024). The total

* Corresponding author e-mail: ebispiadri@gmail.com

thickness of the formations exceeds 450 m in the NE of the SPGF, decreasing to 380 m southward. The K4 reservoir unit, the deepest zone with ~160m thickness, is composed of limestone and dolostone and is characterized by high porosity values (up to 15%), and the highest hydrocarbon productivity (Rahimpour-Bonab et al, 2009). The K3 reservoir unit, with a gross thickness of 120 m, is dominated by dolostones with interlayers of anhydrite. Its lower part is recognizable by thick anhydrite and anhydritic carbonate (up to 50 m) which acts as a hydrocarbon barrier and separates this unit from the K4 (Shahkaram et al. 2022). This barrier interval is equivalent to the dense Upper Anhydrite unit (UA) in the North Field (Esrafili-Dezaji & Rahimpour-bonab, 2009). The K2 reservoir unit consists of ~ 42m productive limestone with a wide range of porosity and permeability values. The base of this unit is defined by a thick thrombolytic facies, which serves as a marker for the Permian-Triassic boundary in the area. This boundary is regarded as an important unconformity representing a significant time missing (Fakhar et al. 2022). The K1 reservoir unit is made up of ~ 100m dolostone with some anhydrite and carbonate intervals at its base. This unit is overlain by the Dashtak Formation (the cap rack of the field).

From a reservoir quality point of view, the K4 and K2 units have good reservoir quality, while the other two are less important. Reservoir quality and the thickness of the formations decrease from NW to SE (Fig. 2). Despite the numerous studies on the Kangan and Dalan formations in the area, their original geologic framework model, lithofacies distribution and internal facies/facies association geometry are not understood yet.

This study focuses on these aspects and their application in reservoir modeling of the SPGF. The primary goals involve reservoir modeling of the formations and mapping the distribution of facies associations across the entire field. Due to the limitation of the available cores for the facies/facies association analysis, an integrated (petrography and geostatistical) approach, using a Self Organizing Map (SOM) neural network is planned to construct an improved reservoir model of the studied succession. The facies and facies associations of the formations have been identified based on the cores from three cored wells. The neural network extends the results obtained from core descriptions to wells with wireline log data. Geo-statistical techniques accomplish modeling of facies and facies associations. Distribution of facies and facies associations are shown throughout the field using distinct codes for each (Qi et al 2007, Iloghalu, E., 2003; Koehrer et al 2010; Lopez et al., 2024).

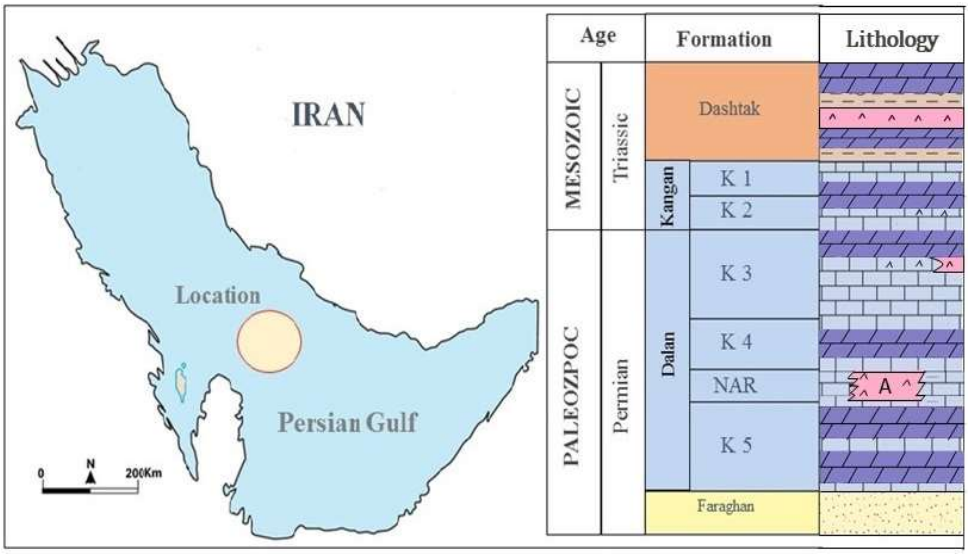

Figure 1. Location map of the SPGS in the Persian Gulf (right) and its general stratigraphy (left)

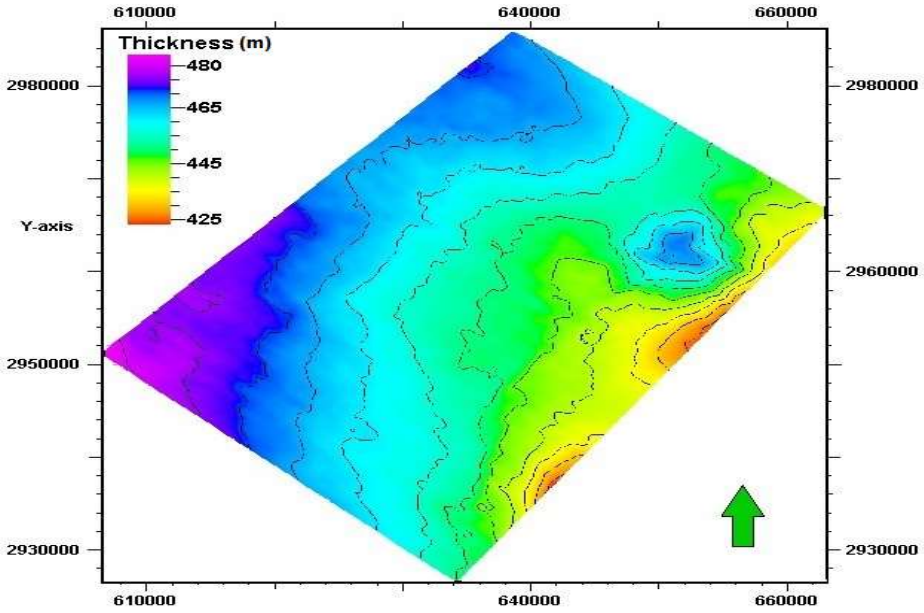

Figure 2. Isopach map of the studied formations in the South Pars Gas Field

Material and Methods

This study focuses exclusively on the geological facies modeling (facies defined from cores, cuttings, and logs) of the studied formations to address the modeling and simulation of the best reservoir interval(s). The research incorporates cores from three key wells containing standard thin sections and core-measured porosity and permeability values. Wireline logs, reservoir tops, and the UGC map of the reservoir horizons were available for this study. Petrographic analysis of 1800 thin sections from a 1000 m core was a base of facies and facies association determination.

In the cored wells, the facies were determined based on texture, size, type of the allochems (ooids, peloids, shell fragments, etc.), matrix and cement types, and diagnostic sedimentary features. Substantial diagenetic features and their effects on porosity evolution are also considered. Compared with the standard microfacies (Flugel, 2010), the facies with similar characteristics are grouped as facies associations (FAs) and linked to specific depositional environments (c.f. Wilson, 1975; Flugel, 2010). These facies were used as a base for predicting lithofacies (logfacies of Serra, 1986) in the uncored wells through the Neural Network approach (Sfidari et al., 2012; Qi et al., 2007). The predicted lithofacies were cross-validated with the core-determined facies using the Neural Network approach and then employed for facies modeling through the Geostatistical method (Fig. 3).

In the uncored wells, a suite of well logs - gamma ray (GR), acoustic transmit-time (DT), neutron (NPHI), density (RHOB), and photoelectric log (PEF) - were selected for logfacies analysis. Therefore, the facies in the uncored wells were predicted based on their characteristics in these logs, while correlating with facies defined from the cores. The predicted lithofacies with similar characters were also grouped in lithofacies associations (LFAs). During the correlation of predicted lithofacies and LFAs with the core-defined facies and FAs, depth matching was performed to ensure accurate alignment of well log data with the corresponding fine-scale core data.

Facies analysis, Litho-facies Prediction, and Depositional Model

A combination of core description and petrographic studies identified 12 facies, with their major

characteristics shown in Table 1. Results from all previous studies on the facies analysis of these formations (e.g., Insalaco et al., 2006; Ehremberg, 2007; Rahimpour-Bonab et al., 2009; Esrafili-Dizaji & Rahimpour-Bonab, 2009; Rahimpour-Bonab et al., 2010; Tavakoli et al., 2011; Tavakoli & Rahimpour-Bonab, 2012; Moradi et al., 2024) were also considered to achieve a more comprehensive and practical classification of the facies.

Table 1. Major facies of the studied formations, their sedimentological composition, and depositional environment

Facies number	Facies name	Depositional environment	Lithology	Texture	Allochem	Energy level	SMF Equal
CF-1	Anhydritic mudstone	Supra tidal	Anhydrite	Mudstone	No Allochem	Low	RMF 25
CF-2	Stromatolite Boundstone	Intertidal	carbonate	Boundstone	Microbial Organism	Low	RMF 20
CF-3	Pelloidal Grainstone	Intertidal lagoon	carbonate	Grainstone	Pelloid, Ooid	Medium	RMF 20
CF-4	Muddy Anhydrite	Lagoon	Carbonate, Anhydrite	Wackstone, Packstone	Gastropode, Pelloid	Low	RMF 22
CF-5	Bioclast Wackeston To Packstone	Lagoon	Carbonate/ Dolomite	Wackstone, Mudstone	Green Algae, Benthic Foraminifer	Low	RMF 22
CF-6	Fossiliferous Lime Mudstone	Lagoon	Carbonate/ Dolomite	Mudstone	Milliolid, Gastropode	Low	RMF 18
CF-7	Ooid Grainstone	Shoal	Carbonate/ Dolomite	Grainstone	Ooid, Bioclast	Medium	RMF 15
CF-8	Bioclast Grainstone	Shoal , Lee ward		Grainstone	Bioclast, Pelloid	High	RMF 17
CF-9	Bioclast Grainstone	Shoal, Sea ward	carbonate	Grainstone	Bioclast, Pelloid	High	RMF 12
CF-10	Intraclast Grainstone	Shoal	Limestone	Grainstone	Ooid, Intraclast	High	RMF 15
CF-11	Dolostone	Shoal	Dolomite	Grainstone	Bioclast Pelloid Intraclast	High	RMF 13
CF 12	Bioclast Wackstone	Open Marine	carbonate	Wackstone	Brachiopode, Bioclast	Medium	-

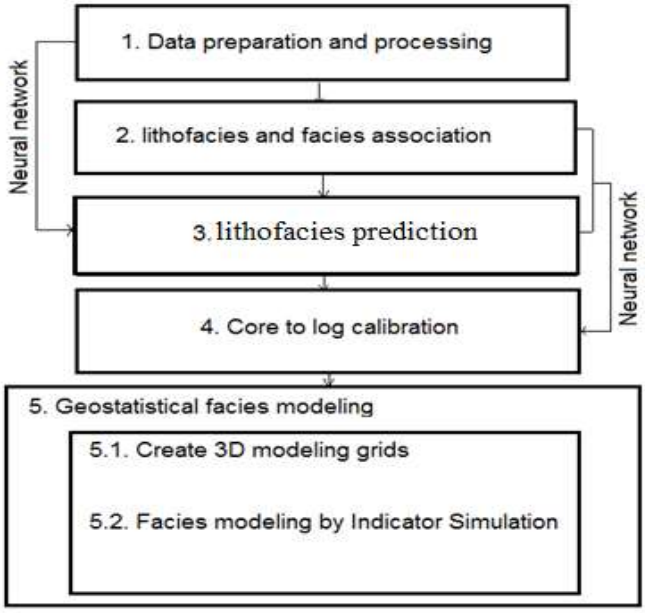

Figure 3. Flowchart illustrating the major steps used in modeling and simulation of the geological facie

Facies analysis in the uncored wells was carried out by lithofacies prediction from wireline logs. Application of computational (artificial) intelligence and pattern recognition to predict lithofacies from wireline logs is well-documented in numerous publications (e.g., Derek et al., 1990; Wong et al., 1995; Saggaf & Nebrija, 2003; Iloghalu, 2003; Qi et al., 2006; Dubois et al., 2007; Al-Anazi & Gates, 2010; Dashti et al., 2016; Maahs et al., 2024; Norsahminan et al., 2024). Transforming lithofacies from logfacies or predicting from wireline logs is a key element in field-scale studies (Qi et al., 2006; Maahs et al., 2024; Norsahminan et al., 2024). The transformation is very challenging due to the non-linear relationship between the fine-scale described lithofacies and the coarse-scale wireline log data. A crucial aspect of this approach is that the wireline logs are used as input data, with each lithofacies serving as a separate target input into the ANN.

The electrofacies/logfacies analysis of the formations in the studied area is well documented in Sfidari et al., 2012a, 2012b. The initial results of extracted lithofacies from the determined logfacies were unreliable due to the discrepancies in calibration from logfacies to lithofacies in mud support intervals. To address this, a successful single-layer neural network (NN) with a backpropagation algorithm was used to predict lithofacies classes from normalized digital well logs. This approach (model) was trained, validated, and tested in the three key wells by correlating the predicted lithofacies with facies determined from the cores (Fig. 4).

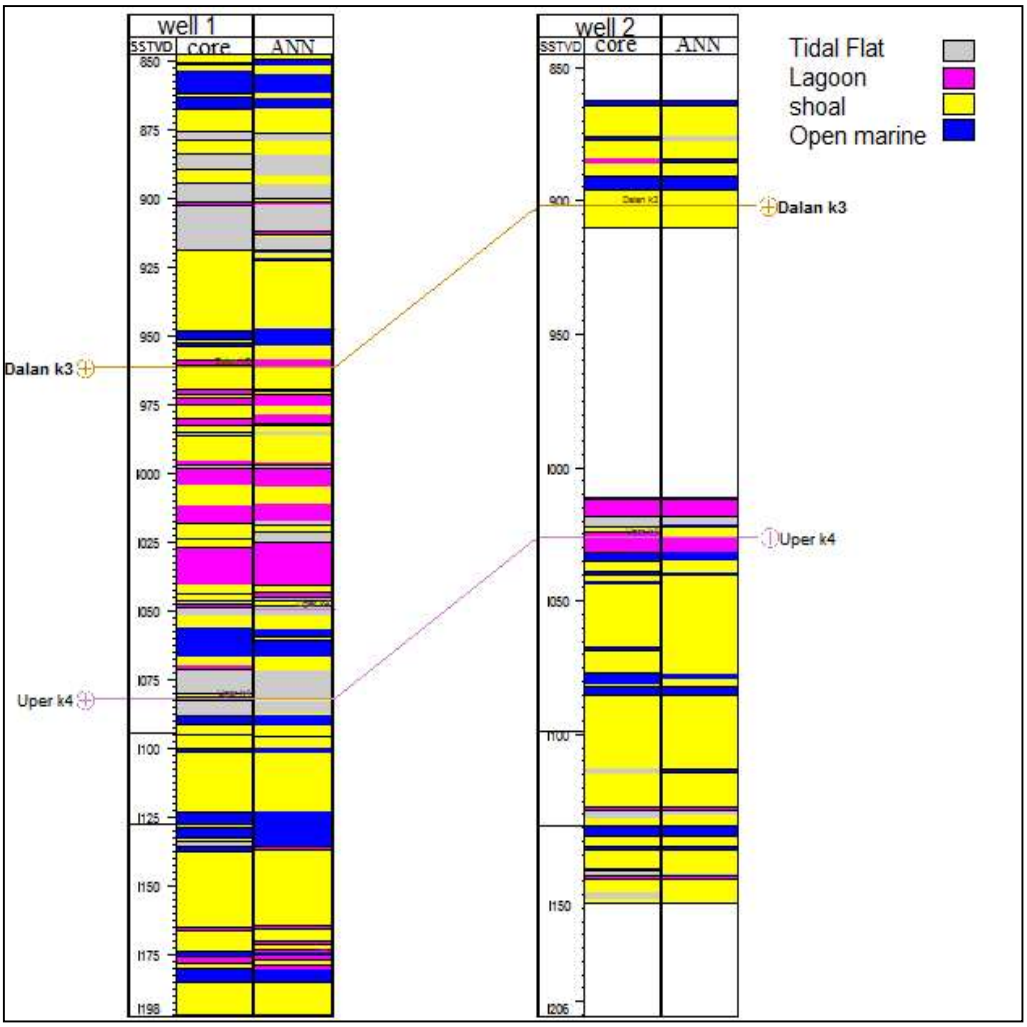

Figure 4. Prediction of litho-facies associations by the Neural Network model in two key wells of the SPGF

The model, fine-tuned with parameters from crass validation and testing (network size and damping parameter), was subsequently used for lithofacies prediction in the uncored wells. Similarly, the model was applied to predict the lithofacies associations (LFAs) in the uncored wells of the field. Results displayed a good performance and a reliable prediction of the Neural Network classification (Table 2).

The depositional environments of the facies were determined based on their sedimentological characteristics (Table 1), their vertical and lateral extents, their comparison to the standard microfacies (Flugel, 2010), and those reported from equivalent formations in the area (e.g., Al-Aswad, 1997; Angiolini et al., 2003; Alsharhan & Kendall, 2003; Khalifa, 2005; Alsharhan, 2006). Based on their main characteristics, the facies are classified into four facies associations - tidal flat, lagoon, shoal, and open marine - on a carbonate ramp (Fig. 4). Depositional environments of the formations in the uncored wells were discussed through correlation of the predicted lithofacies and LFAs with the facies associations defined on the cores (table 3). The lateral distribution of facies associations and their counterparts (LFAs) across the field indicates a wide carbonate ramp along the south margin of the Neo Tethys. The absence/scarcity of reef deposits and the low diversity of facies types confirm this indication (Ahr, 1973; Burchette & Wright, 1992; Avrell et al., 1998). Similar conditions have been reported for equivalent deposits (Khuff Formation) in neighboring areas (Al-Aswad, 1997; Alsharhan, 2006).

The Lime mudstones with anhydrite patches (facies 1) and stromatolite boundstones with wackestone to packstones (facies 2) characterize the lower sabkha to high energy parts of the lower tidal flat. Restricted and harsh conditions in the tidal flat most likely led to increased salinity and sporadic development of evaporites (facies 1).

Table 2. The prediction effectiveness of the Neural Network classification model for Kangan and Dalan formations of the SPGF, SW Iran (Neural network size: 20; damping parameter: 0.01; iteration number: 500)

Confusion matrix		predicted litho-facies					Absolute accuracy
		1	**2**	**3**	**4**	**Grand Total**	
Actual facies	1	**212**	13	45	4	274	77.372
	2	7	**273**	31	2	313	87.220
	3	40	29	**981**	27	1077	91.086
	4	11	1	15	**109**	136	80.147
	Grand Total	270	316	1072	142	1800	
	Proportion percent (%)	98.540	100.958	99.535	104.411		Absolute accuracy
	difference	4	3	5	6	18	87.500

Table 3. Predicted LFAs, their lithology, equivalent FA, and depositional setting

Lithofacies associations	lithology	Equ. FA	Environmental conditions
LFAs 1	dolomudstone with anhydrite patches, micritic and stromatolite layers	FA -1	Tidal flat
LFAs 2	wackestone to packstones, microcrystalline dolomite and anhydrite patches	FA-2	Lagoon
LFAs 3	Well-sorted oolitic, bioclast to intraclasts grainstone, highly porous	FA-3	Shoal
LFAs 4	Fine-laminated argillaceous limestones, Lime mudstone to wackestones	FA-4	Open marine

Fenestral fabrics and keystone vugs remark the mudstone/wackestones of the middle and lower intertidal zone. Facies 3, 4, 5, and 6 characterize restricted sub-environments (lagoons) formed landward of the shoal barriers with low energy, low biodiversity, and temporal high salinity conditions. Water restriction was most likely affected by the efficiency of the shoal complex in time and space. The facies 7, 8, 9, 10, and 11 represent barrier shoals, the high-energy parts of the ramp, and are the most significant facies in the studied formations due to their high porosity and permeability. Facies 12 (Bioclast Wackstone) is related to fore shoals or open marine settings of the ramp (below storm wave base), based on their sedimentological and faunal features.

Reservoir Quality

The petrophysical characteristics of the facies and facies associations were determined in the cored wells from core-measured porosity and permeability. Then, the results were extended to predicted lithofacies and LAFs in the uncored wells (Dashti et al., 2016; Sfidari et al., 2018, 2021). By examining the relationships between facies and their reservoir quality, the paleo-environmental control on the petrophysical properties of the facies and predicted lithofacies was inferred. This assessment uncovered that the most potential pore spaces are observed in grain-dominated facies related to the high-energy shoal setting (Fig. 5).

In most facies of this setting, porosity and permeability values vary from 0 to 35% and 0 to 500md respectively (Figs. 5 & 6). The pore spaces are predominantly inter-particle, with some moldic type. A linear relation between porosity and permeability of these facies indicates the significant role of depositional conditions on reservoir quality. Analysis of porosity distribution in the predicted lithofacies and LFAs in the uncored wells provide comparable results (Fig 6).

Three-Dimensional Modeling

The 3D model of the studied formations was established based on the spatial distribution of their constituent LFAs, the nature of the depositional setting, and the stratigraphic framework (Dashti et al., 2016; Maahs et al., 2024; Norsahminan et al., 2024). A three-dimensional UGC map of top K1 was available for this study.

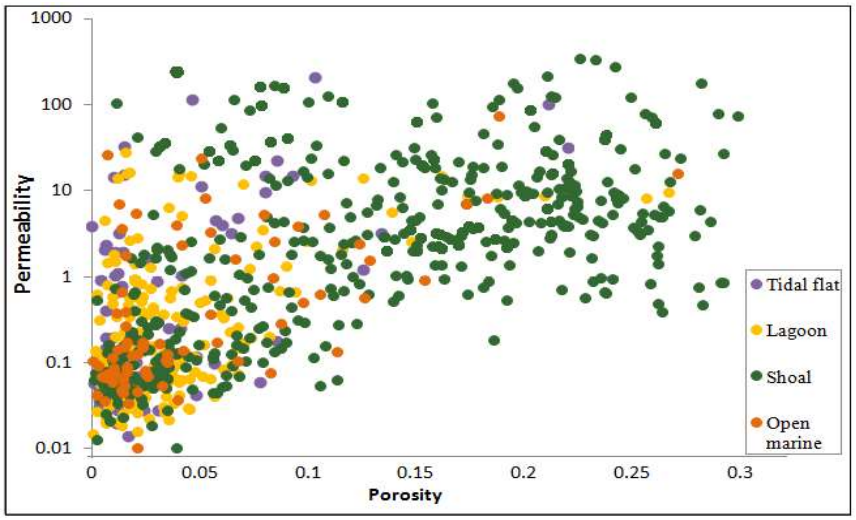

Figure 5. Porosity-permeability cross-plot of the studied facies associations, indicating the highest reservoir quality in the shoal FA. The poor quality of some facies in this setting is due to the pervasive diagenetic features

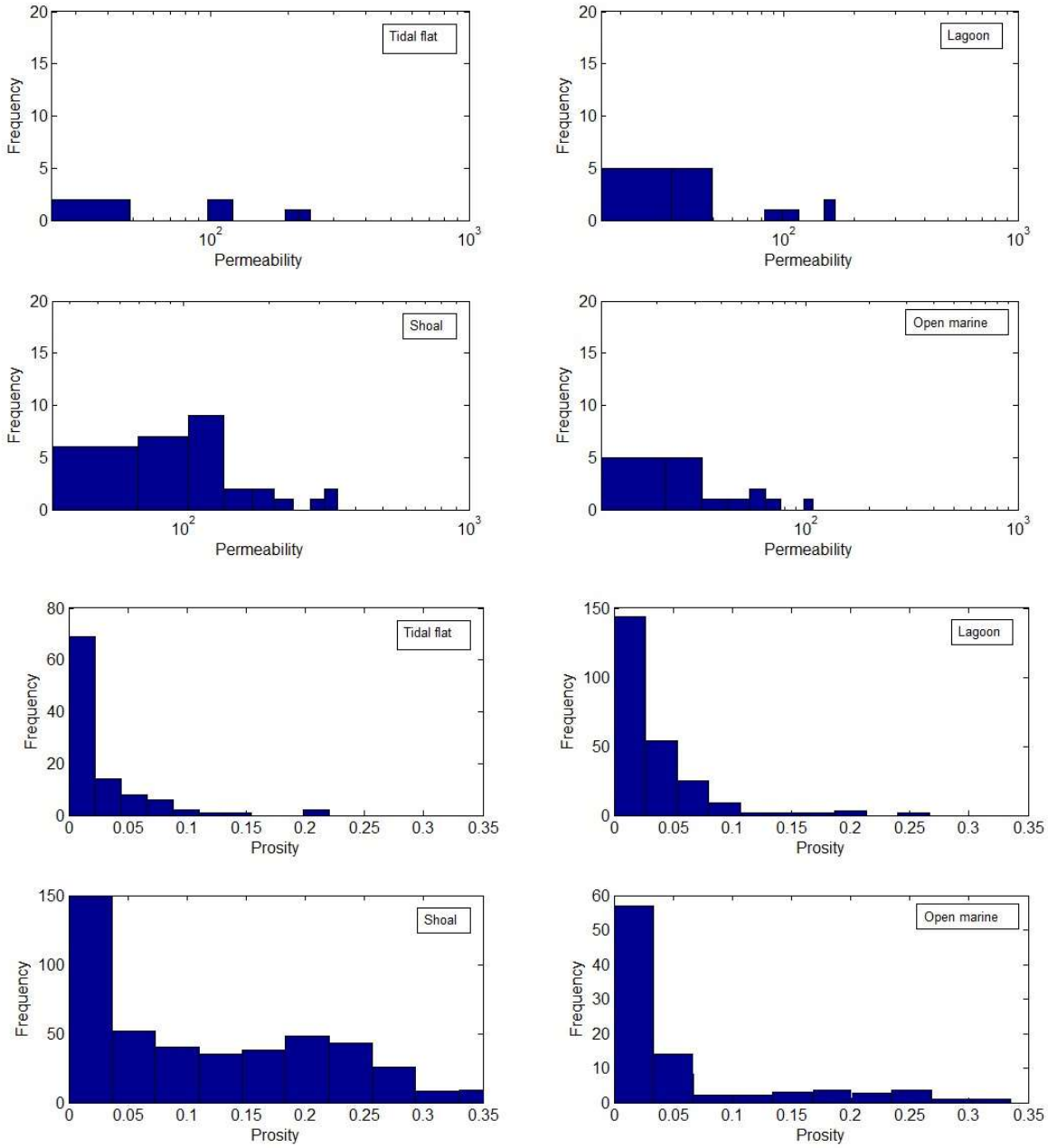

Figure 6. Porosity and permeability distribution in the studied LFAs

The other four structural surfaces (top K2, K3, K4, and Nar anhydrite) were built based on this surface, given no major fault effects (Asadi-Eskandar et al., 2013). The top K1 and top Nar anhydrite were selected as the upper and lower boundaries of the studied succession model, respectively. The five structural surfaces - top K1, K2, K3, K4, and Nar anhydrite - were used as the framework for the modeling, resulting in four sub-grids (the main reservoir zones). The horizontal dimensions of the model were 60 × 68 km in the Y and X directions, respectively. The 3D model comprises 16320 grid cells with lateral dimensions of about 500 × 500 m. The further subdivision of the model in vertical scale is 300 layers with a 1 m resolution grid (Fig. 7).

The spatial distribution of the LFAs and the geometry of the depositional model are properly understood by geostatistical analysis of the model (c.f. Dubrule, 1998; Deutsch, 2002; Dashti

et al., 2016; Maahs et al., 2024; Norsahminan et al., 2024). The stochastic simulation method, also known as sequential indicator simulation and kriging was applied here to simulate and generate the 3D model of the studied succession. The four major LFAs were involved in the modeling representing tidal flat (LFAs 1), lagoon (LFAs 2), shoal (LFAs 3), and open marine (LFAs 4) environments.

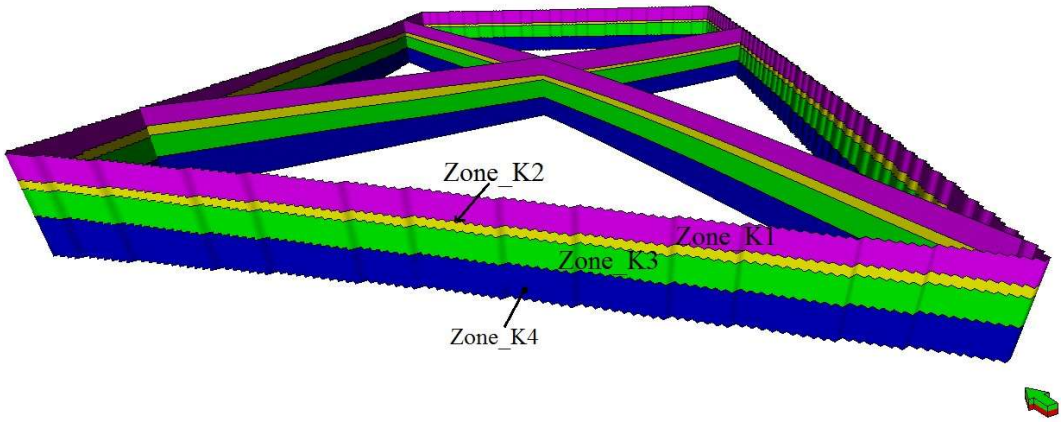

Figure 7. Three-dimensional intersection of the four main sub-grid reservoir zones, as a fundamental stratigraphic framework for subsequent simulating of the litho-facies associations

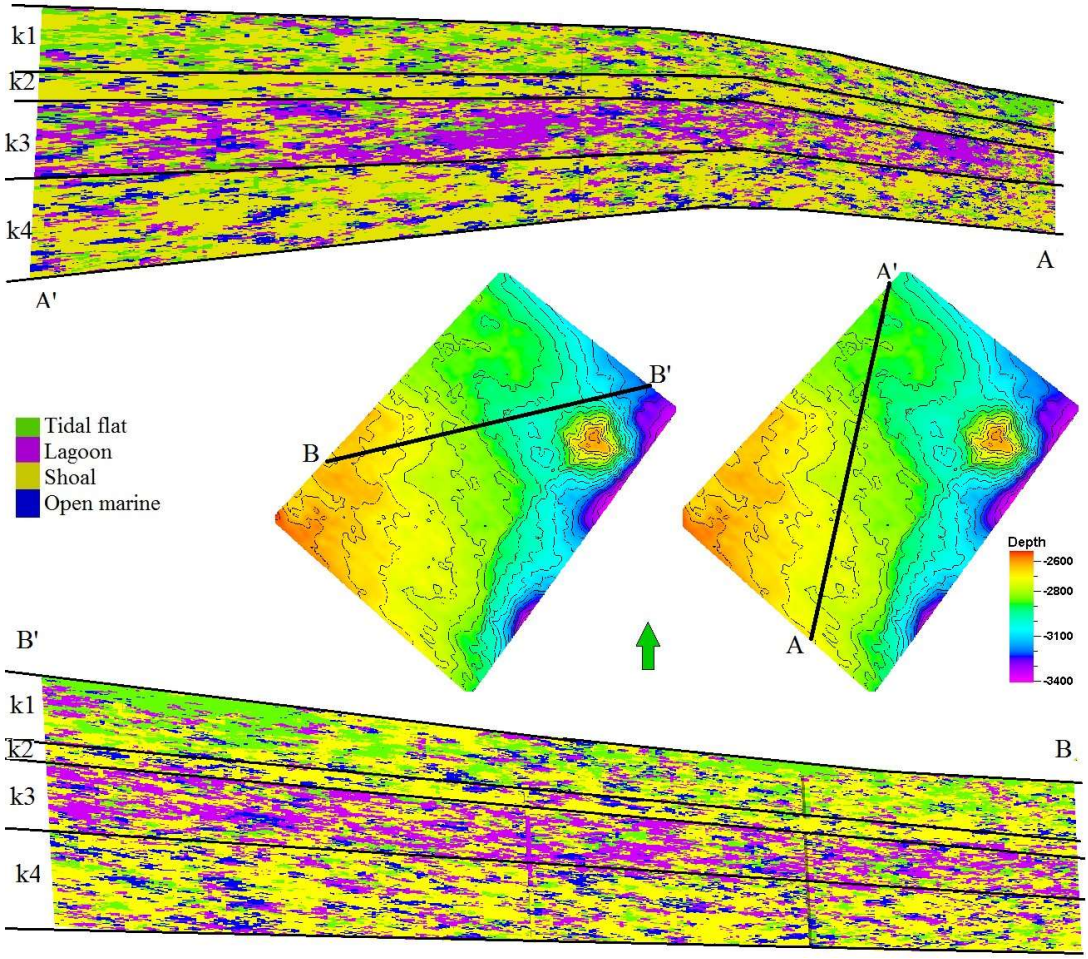

Figure 8. Cross-section of the lithofacies associations modeled in the studied field

The sequential indicator simulation is based on the indicator approach (Journel, 1983; Gomez-Hernandez & Srivastava, 1990). This method is one of the most popular approaches, as a pixel-based modeling algorithm, in producing multiple facies realization. This approach attempts to model the facies/lithofacies based on a variogram that represents the size and frequency of the facies. The experimental variograms were first calculated from the facies curve in the wells. After that, the experimental variograms were fitted to the variogram model to get the horizontal and vertical of the facies (Table 4). As a final point, the simulation was performed by the use of simple kriging (Figs. 8-10).

Facies modeling of the formations indicates a gentle shallowing from zone K4 to zone K3. The connectivity of shoal facies (LFAs 3) is well observed in zone K4, whereas in zone K3 the connectivity of LFAs 2 (lagoon facies) is evident (Figs. 8-10). This trend, indicative of shallowing in depositional settings, is associated with a decrease in reservoir quality from K4 to K3. Zone K2 is characterized by dominant LFAs 3 (shoal) and minor LFAs 4 (open marine) (Figs. 8-10). Compared to zone K3, a gentle deepening in the depositional environment is evident, which is associated with greater connectivity of shoal facies NW ward, hence better reservoir quality.

Table 4. Variogram data of the main facies associations/LFAs of the studied formations. These data were used for 3D facies modeling by indicator simulation

LFAs	Variogram			azimuth	Variogram type
Tidal flat	2500	1800	11	43	Exponential
Lagoon	2700	1700	17	43	Exponential
Shoal	3000	1900	21	43	Exponential
Open marine	2400	1600	13	43	Exponential

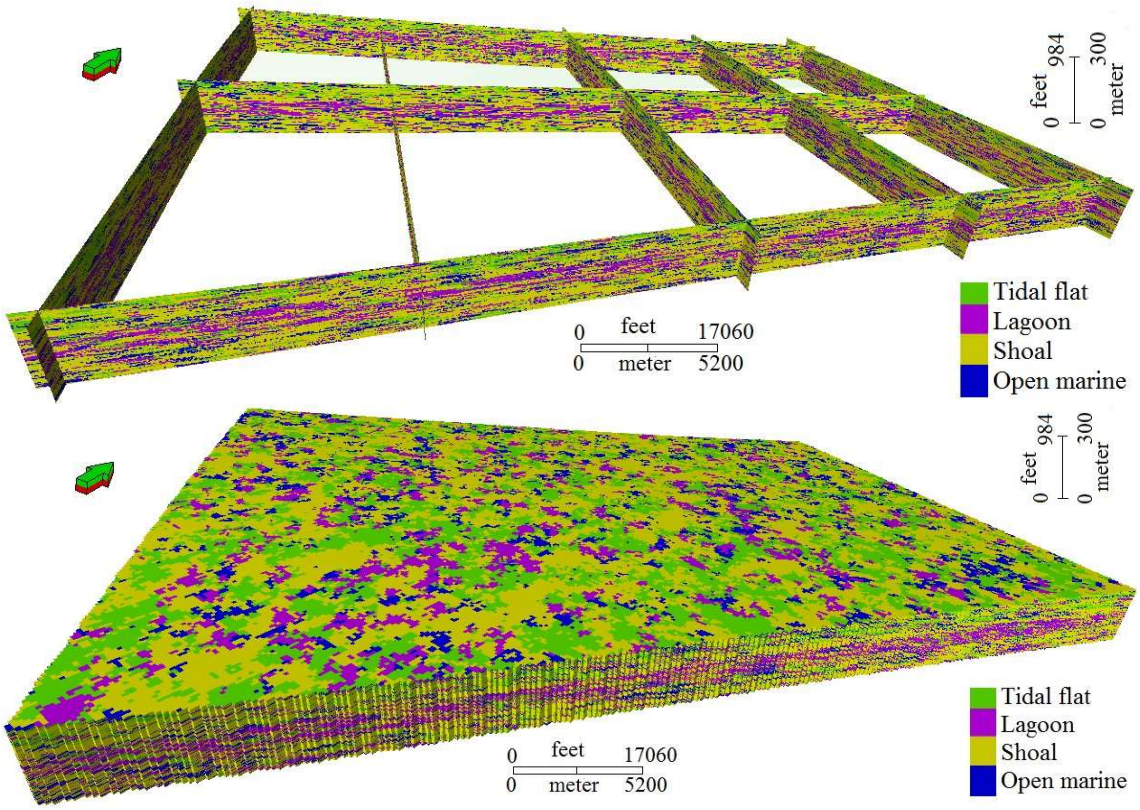

Figure 9. Facies model based on indicator simulation with kriging. The block model of the entire field (top) and 3D cut slice in the x and y axis (below). Vertical exaggeration is X5

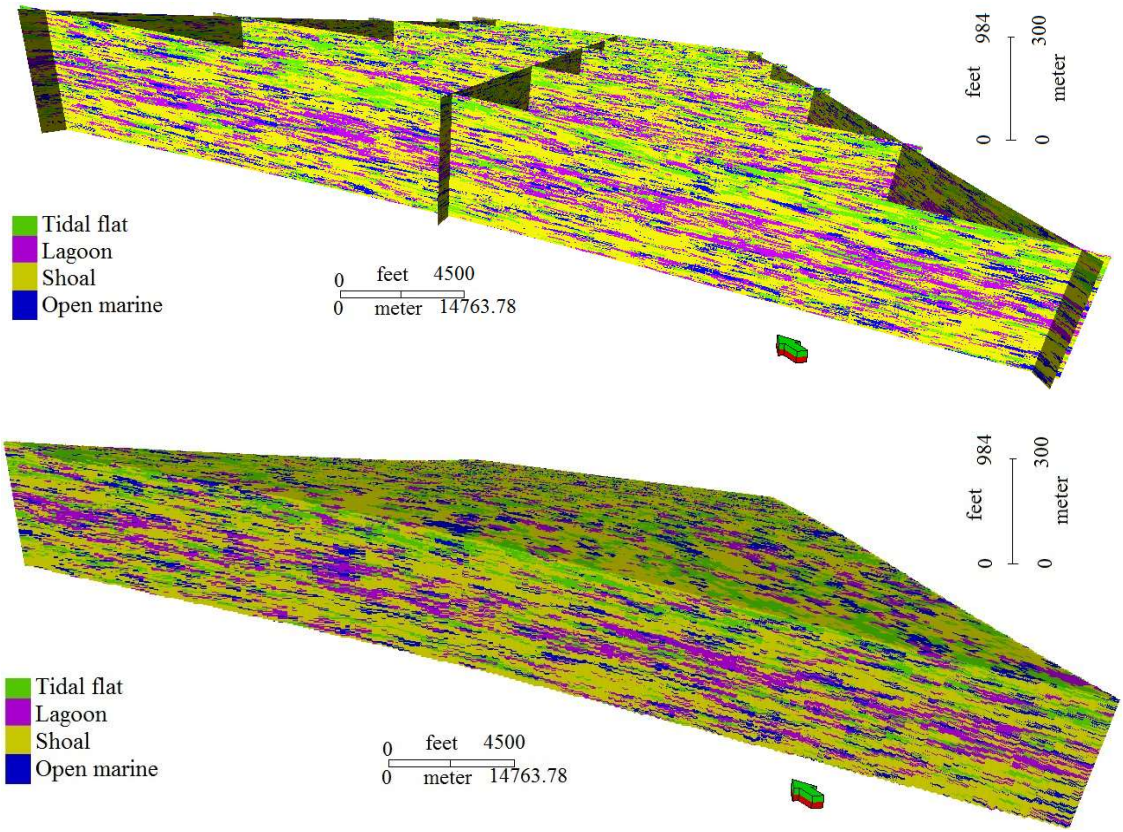

Figure 10. Facies model based on indicator simulation with kriging. The block model of the field (top) and 3D cut slice in the x and y axis (below). Vertical exaggeration is X15

Zone K1 is characterized by the dominance of LFAs 1 (tidal flat facies). Compared to zone K2, a gentle shallowing in the depositional environment and a decrease in reservoir quality are observed. Considering the age of the studied zones (Fig. 1), a 2nd-order relative sea-level fall during the development of the zones (from K4 to K1) is understandable from facies modeling of the formations (Figs. 8-10).

Conclusions

The calibration of petrographic and wireline log data with rock types by an Intelligent Neural Network approach establishes a reliable framework for reservoir modeling. This model provides significant information on the depositional setting, diagenesis, and the vertical and lateral distribution of the reservoir facies.

Twelve facies are identified and classified into four facies associations representing tidal flat (LFAs 1), lagoon (LFAs 2), shoal (LFAs 3), and open marine (LFAs 4) conditions on a carbonate ramp. Indicator simulation with kriging, based on the predicted lithofacies from wireline logs, is applicable for facies modeling and discriminating reservoir zones in the studied formations.

Substantial core data was required to validate the predicted lithofacies from wireline logs. The neural network method is a great help in correlating log-derived facies with core-based facies.

The dominance of the LFAs 3 (shoal facies) in the studied formations plays a significant role in their high reservoir quality. So, depositional conditions are the main controls on the reservoir quality of the formations, although diagenetic processes are considerable.

The neural network and pattern recognition method successfully predicted lithofacies in uncored wells, with absolute accuracy ranging from 77% for LFAs 1 to 91% for LFAs 3, and an average accuracy of 87%.

Facies modeling based on indicator simulation with kriging can be used for relative sea level change analysis, especially where the core-derived data are limited.

Facies modeling of the formations indicates a gentle shallowing trend from zone K4 to zone K3. The connectivity of LFAs 3 is well observed in zone K4, whereas in zone K3, LFAs 2 connectivity is evident. Zone K2 is characterized by dominant LFAs 3 and minor LFAs 4, while zone K1 is dominated by LFAs 1.

Acknowledgments

The authors express their sincere gratitude to the geology department of POGC for providing the data utilized in this study.

References

Ahr, W.M., 1973. The carbonate ramp: an alternative to the shelf model. Trans-Gulf Coast Association of Geological Society, 23: 221-225.

Al-Anazi, A., Gates, I. D., 2010. A support vector machine algorithm to classify lithofacies and model permeability in heterogeneous reservoirs, Engineering Geology, 114: 267-277.

Al-Aswad, A., 1997. Stratigraphy, sedimentary environment and depositional evolution of the Khuff Formation in south-central Saudi Arabia. Journal of Petroleum Geology, 20: 1-20.

Alsharhan, A.S., Kendall, C.G. St.C., 2003. Holocene coastal carbonates and evaporates of the southern Arabian Gulf and their ancient analogues. Earth-Science Reviews, 61: 191-243.

Alsharhan, A.S., 1993. Facies and sedimentary environment of the Permian carbonates (Khuff Formation) in the United Arab Emirates. Sedimentary Geology, 84: 89-99.

Alsharhan, A.S., 2006. Sedimentological character and hydrocarbon parameters of the middle Permian to Early Triassic Khuff Formation, United Arab Emirates. Geo- Arabia, 11: 121-158.

Angiolini, L., Balini, M., Garzanti, E., Nicora, A., Tintori, A., Crasquin, S., Muttoni, G., 2003. Permian climatic and paleogeographic changes in the Northern Gondwana: The Khuff Formation of interior Oman, Paleogeography, Paleoclimatology, Palaeoecology, 191: 269-300.

Arab Oil and Gas Magazine, 2003. South Pars production above target rate with only 15 of the 20 planned wells drilled. The Arab Petroleum Research Center. AOGM, 14-16.

Asadi-Eskandar, A., Rahimpour-Bonab, H., Hejri, S., Afsari, K., Mardan, A., 2013. Consistent Geological-Simulation Modeling in Carbonate Reservoirs, a case study from the Khuff Formation, Persian Gulf. Journal of Petroleum Science and Engineering. (in press).

Avrell, M., Bádenas, B., Bosence, D.W.J., Waltham, D.A., 1998. Carbonate production and offshore transport on a late Jurassic carbonate ramp (Kimmeridgian, Iberian basin, NE Spain): evidence from outcrops and computer modelling. In: Wright, V.P. & Burchette, T.P. (Eds) Carbonate ramps. Geological Society of London, Special Publications, 149: 137-161.

Burchette, T.P., Wright, V.P., 1992. Carbonate ramp depositional systems. Sedimentary Geology, 79: 3-57.

Dashti, A., Ebrahim, S., 2016. Physical properties modeling of reservoirs in Mansuri oil field, Zagros region, Iran. Petroleum Exploration and Development, 43(4): 611-615.

Derek, H., Johns, R., Pasternak, E., 1990. Comparative study of a back propagation neural network and statistical pattern recognition techniques in identifying sandstone lithofacies. Proceedings 1990Conference on Artificial Intelligence in Petroleum Exploration and Production. Texas A and M University, College Station, TX, 41-49.

Deutsch, C. V., 2002. Geostatistical Reservoir Modeling (Applied Geostatistics Series). Oxford, New York.

Dubois, M, K., Bohling, G, C., Chakrabarti, S., 2007. Comparison of four approaches to a rock facies classification problem, Computers and Geosciences, 33 (5): 599-617.

Dubrule, O., 1998. Geostatistics in petroleum geology, AAPG Special, 38.
Ehrenberg, S. N., Nadeau, P. H., Aqrawi, A. A. M., 2007. A comparison of Khuff and Arab reservoir potential throughout the Middle East. AAPG Bulletin, 91: 275-286.
Esrafili-Dizaji, B., Rahimpour-Bonab, H., 2009. Effects of depositional and diagenetic characteristics on carbonate reservoir quality: a case study from the South Pars Gas field in the Persian Gulf. Petroleum Geoscience, 15: 325-344.
Fakhar, M., Rezaee, P., Karimian, A., 2022. Microfacies, depositional environment, and sequence stratigraphy of the carbonate-evaporate successions of the Kangan Formation in the central part of the Persian Gulf. Journal of Stratigraphy and Sedimentology Researches University of Isfahan, 115-146.
Flugel, E., 2010. Microfacies Analysis of Carbonate Rocks. Analyses, Interpretation and Application. Springer Verlag, 976 pp.
Ghazban, F., 2007. Petroleum Geology of the Persian Gulf. Adviser: H. Motiei. University of Tehran press, 707 pp.
Gomez-Hernandez, J., Srivastava R. M., 1990. ISIM 3D: An ANSI-C three-dimensional and multiple indicator conditional simulation programs: Computers and Geosciences, 16: 355-410.
Iloghalu, E., 2003. Application of neural networks technique in lithofacies classifications used for 3-D reservoir geological modeling and exploration studies. AAPG Annual Meeting Abstract.
Insalaco, E., Virgone, A., Courme, B., Gaillot, J., Kamali, M., Moallemi, A., Lotfpour, M., Monibi, S., 2006. Upper Dalan Member and Kangan Formation between the Zagros Mountains and offshore Fars, Iran: Depositional system, biostratigraphy and stratigraphic architecture. GeoArabia, 11: 75-176.
Journel, A. G., 1983, Nonparametric estimation of spatial distributions: Mathematical Geology, 15: 445-468.
Kalhori, M., Mehrabi, H., Sfidari, E. and Khiabani, S.Y., 2024. Target zone selection for hydraulic fracturing using sedimentological and rock mechanical studies with the support of the machine learning method of cluster analysis. Geoenergy Science and Engineering, 237, 212826.
Khalifa, M.A., 2005. Lithofacies, diagenesis and cyclicity of the 'Lower Member' of the Khuff formation (late Permian), Al Qasim Province, Saudi Arabia, Journal of Asian Earth Sciences, 25 (5): 719-734.
Koehrer, B.S., Heymann, C., Prousa, F., Aigner, T., 2010. Multiple-scale facies and reservoir quality variations within a dolomite Body-Outcrop analog study from the Middle Triassic, SW German Basin. Marine and Petroleum Geology, 27: 386-411.
López, J.M.P., Poyatos-Moré, M., Howell, J., 2024. Facies analysis and sequence stratigraphy of shallow marine, coarse-grained siliciclastic deposits in the southern Utsira High: The Late Jurassic intra-Draupne Formation sandstones in the Johan Sverdrup Field (Norwegian North Sea). Basin Research, 36(1): p.e12833.
Maahs, R., Kuchle, J., Rodrigues, A.G., Trombetta, M.C., dos Santos Alvarenga, R., Barili, R., Freitas, W., 2024. Three-dimensional geological modeling applied to multiscale heterogeneity of a reservoir analog: paleocoastal deposits from the Rio Bonito Formation, Paraná Basin. Marine and Petroleum Geology, p.106930.
Moradi, M., Kadkhodaie, A., Rahimpour-Bonab, H., Kadkhodaie, R., 2024. Integrated reservoir characterization of the Permo-Triassic gas reservoirs in the Central Persian Gulf. Petroleum.
Norsahminan, D.N.P., Islam, M.A., Thota, S.T., Shalaby, M.R., 2024. 3D reservoir characterization of the Mangahewa Formation, Mangahewa Field, Taranaki Basin, New Zealand. Energy Geoscience, 5(2): 100266.
Qi, L., Carr, T.R., Goldstein, R.H., 2007. Geostatistical three-dimensional modeling of oolite shoal, St. Louis Limestone, southwest Kansas. The American Association of Petroleum Geologists. Bulletin, 91(1): 69-96.
Qi, L.S., Carr T.R., 2006. Neural Network Prediction of Carbonate Lithofacies from Well Logs, Big Bow &Sand Arroyo Creek Fields, Southwest Kansas: Computers and Geosciences, 32: 947-964.
Rahimpour-Bonab, H., 2007. A procedure for appraisal of a hydrocarbon reservoir continuity and quantification of its heterogeneity, Journal of Petroleum Science and Engineering, 58 (1-2): 1-12.
Rahimpour-Bonab, H., Asadi-Eskandari, A., Sonei, A., 2009. Control of Permian-Triassic Boundary over reservoir characteristics of South Pars gas field, Persian Gulf. Geological journal, 44: 341-364.

Rahimpour-Bonab, H., Esrafili-Dizaji, B., Tavakoli, V., 2010. dolomitization and precipitation in permo-triassic carbonates at the South Pars gas field, offshore Iran: controls on reservoir quality, Journal of Petroleum Geology, 33(1): 43 - 66.

Saggaf, M.M., Nebrija E.L., 2003. A fuzzy logic approach for the estimation of facies from wire-line logs: AAPG Bulletin, 87(7): 1233-1240.

Serra, O., 1986. Fundamentals of well log interpretation. Vol. 2: the interpretation of logging data. Elsevier, Amsterdam, 684 pp.

Sfidari, E., Amini, A., Kadkhodaie, A., Ahmadi, B., 2012. Electrofacies clustering and a hybrid intelligent based method for porosity and permeability prediction in the South Pars Gas Field, Persian Gulf, Journal of Geopersia, 2(2): 11-23.

Sfidari, E., Amini, A., Kadkhodaie, A., SeyedAli, M., Seyed Mohammad, Z., 2018. Diagenetic and depositional impacts on the reservoir quality of the Upper Jurassic Arab Formation in the Balal Oilfield, Offshore Iran. Acta Geologica Sinica-English Edition, 92(4): 1523-1543.

Sfidari, E., Kadkhodaie-Ilkhchi, A., Najjari, S., 2012. Comparison of intelligent and statistical clustering approaches to predicting total organic carbon using intelligent systems. Journal of Petroleum Science and Engineering, 86-87, 190-205.

Sfidari, E., Sharifi, M., Amini, A., Zamanzadeh, S.M., Kadkhodaie, A., 2021. Reservoir quality of the Surmeh (Arab-D) reservoir in the context of sequence stratigraphy in Salman Field, Persian Gulf. Journal of Petroleum Science and Engineering, 198: 108180.

Shahkaram, M., Aleali, M., Tavakoli, V., Maleki, Z., 2022. Description and correlation of facies and depositional sequences of Kangan and Dalan formations in Permian-Triassic carbonate ramp, central and eastern Persian Gulf. Applied Sedimentology, 10(19): 186-202.

Shahkaram, M., Aleali, M., Tavakoli, V., Maleki, Z., 2022. Description and correlation of facies and depositional sequences of Kangan and Dalan formations in Permian-Triassic carbonate ramp, central and eastern Persian Gulf. Applied Sedimentology, 10(19): 186-202.

Sharland, P.R., Archer, R., Casey, D.M., Davies, R.B., Hall, S.H., Heward, A.P., Horbury, A.D., Simmons, M.D., 2001. Arabian plate sequence stratigraphy, GeoArabia Spec. Publ., Bahrain Gulf Pet, 2, 374 pp.

Tavakoli, V., Rahimpour-Bonab, H., 2012. Uranium depletion across Permian-Triassic Boundary in Persian Gulf and its implications for paleo-oceanic conditions. Paleogeography, Paleoclimatology, Paleoecology 350-352: 101-113.

Tavakoli, V., Rahimpour-Bonab, H., Esrafili-Dizaji, B., 2011. Diagenetic controlled reservoir quality of South Pars Gas field, an integrated approach. Competes Rendus Geosciences, 343(1): 55-71.

Wilson, J.L., 1975. Carbonate Facies in Geologic History. Springer-Verlag, New York.

Wong, P., Jian, F., Taggart, I., 1995. A critical comparison of neural networks and discriminant analysis in lithofacies, porosity, and permeability predictions. J. Pet. Geol, 18 (2): 191-206.